



## Insights on the conformation and appropriate drug-target sites on retinal IMPDH1 using the 604-aa isoform lacking the C-terminal extension

Parisa Elyasi-Ebli<sup>1</sup>, Razieh Yazdanparast<sup>1,\*</sup>, Sajjad Gharaghani<sup>1</sup>, and Ebrahim Barzegari<sup>1,2,\*</sup>

<sup>1</sup>Institute of Biochemistry and Biophysics, University of Tehran, Tehran, Iran.

<sup>2</sup>Medical Biology Research Center, Health Technology Institute, Kermanshah University of Medical Sciences, Kermanshah, Iran.

### Abstract

**Background and purpose:** Retinitis pigmentosa (RP) accounts for 2 percent of global cases of blindness. The RP10 form of the disease results from mutations in isoform 1 of inosine 5'-monophosphate dehydrogenase (IMPDH1), the rate-limiting enzyme in the *de novo* purine nucleotide synthesis pathway. Retinal photoreceptors contain specific isoforms of IMPDH1 characterized by terminal extensions. Considering previously reported significantly varied kinetics among retinal isoforms, the current research aimed to investigate possible structural explanations and suitable functional sites for the pharmaceutical targeting of IMPDH1 in RP.

**Experimental approach:** A recombinant 604-aa IMPDH1 isoform lacking the carboxyl-terminal peptide was produced and underwent proteolytic digestion with  $\alpha$ -chymotrypsin. Dimer models of wild type and engineered 604-aa isoform were subjected to molecular dynamics simulation.

**Findings/Results:** The IMPDH1 retinal isoform lacking C-terminal peptide was shown to tend to have more rapid proteolysis (~16% digestion in the first two minutes). Our computational data predicted the potential of the amino-terminal peptide to induce spontaneous inhibition of IMPDH1 by forming a novel helix in a GTP binding site. On the other hand, the C-terminal peptide might block the probable inhibitory role of the N-terminal extension.

**Conclusion and implications:** According to the findings, augmenting IMPDH1 activity by suppressing its filamentation is suggested as a suitable strategy to compensate for its disrupted activity in RP. This needs specific small molecule inhibitors to target the filament assembly interface of the enzyme.

**Keywords:** Inosine monophosphate dehydrogenase; Molecular dynamics simulation; Proteolytic digestion; Retinal isoforms; Retinitis pigmentosa.

### INTRODUCTION

Retinitis pigmentosa (RP) is an acquired and inherited blindness, with 13, 21, and 5 genes reported to date to cause its autosomal dominant, autosomal recessive, and x-linked forms, respectively. The gene *RP10* encodes the isozyme 1 of inosine 5'-monophosphate dehydrogenase (IMPDH1), mutations of which account for the RP10 autosomal dominant form of RP (1). IMPDH1, the rate-limiting enzyme in the purine nucleotide *de novo* synthesis

pathway, catalyzes the conversion of IMP to xanthosine monophosphate using nicotinamide adenine dinucleotide as a cofactor (2,3). In *Mus musculus*, in addition to the canonical isoform of IMPDH1 containing 514 amino acids (aa), there are retinal isoforms containing 546 and 604 aa. The isoform 546 has a 32-aa peptide in the carboxyl-terminal of the protein sequence.

\*Corresponding authors:

R. Yazdanparast, Tel: +98-2166956976, Fax: +98-2166404680

Email: ryazdan@ut.ac.ir

E. Barzegari, Tel: +98-8334276473, Fax: +98-8334276471

Email: e.barzegari@kums.ac.ir

#### Access this article online



Website: <http://rps.mui.ac.ir>

DOI: 10.4103/1735-5362.389951

The isoform 604 contains an extra 57-aa peptide in the amine terminal, in addition to the carboxyl-terminal peptide present in isoform 546. Human orthologues of these three isoforms contain 514, 546, and 595 aa, respectively (4,5).

The structure of IMPDH1 consists of a catalytic domain with  $(\beta/\alpha)_8$  or triosephosphate isomerase (TIM) barrel conformation and two tandem cystathione  $\beta$ -synthase (CBS) subdomains. The active site of the enzyme includes Cys319, located at the carboxyl end of the  $\beta$ -sheets in a GIGPGSICTT motif (6-8). The catalytic flap, a twisted  $\beta$ -sheet on the C-terminal of the catalytic domain, is of assistance in the formation of a pseudo barrel in the octameric conformation of the enzyme. It is encompassed between  $\alpha 8$  and  $\beta 8$  of the catalytic barrel and contains two crucial amino acids, Arg418 and Tyr419, which contribute to the activation of a water molecule essential for IMPDH catalytic activity (9,10). The regulatory CBS subdomains, which also mediate the formation of IMPDH octameric structures, include three nucleotide binding sites. The combination of ATP or GDP/GTP molecules binding to these binding sites has proven to play a key role in the attenuation or elevation of the catalytic activity of the enzyme (11-13). It has been noted that occupation of second and third binding sites by GDP/GTP molecules results in a decrease in catalytic activity (11,12). Moreover, the most prevalent RP-related mutations in IMPDH1, *i.e.* R224P and D226N (human IMPDH numbering; equivalent to R226P and D228N in *Mus musculus*) locate in the nucleotide binding sites of the CBS2 subdomain (11).

In our previous study on the structural properties of the retinal isoforms of IMPDH1, the possible role of C/N-terminal peptides in the regulation of the catalytic activity has been denoted (14). In a recent study, the human IMPDH 595-aa isoform lacking the carboxyl-terminal peptide showed a three-fold decrease in GTP sensitivity due to the formation of the filaments. This study pointed out the filamentation characteristics as the main factor of inhibition and catalytic activity variation in the wild-type and engineered protein (15).

Nimmegern *et al.* performed proteolysis of IMPDH2 in free and substrate-bound states,

concluding that an unbound state of IMPDH2 was more susceptible to protease activity than the substrate-bound states (16). The present study aimed to investigate the unidentified internal interactions in the presence and the absence of the C-terminal peptide of the murine retinal 604-aa isoform. Possible conformational changes caused by the C-terminal peptide were studied by comparing the proteolytic digestion patterns of the recombinant and the wild-type 604-aa isoform. Furthermore, due to lacking X-ray crystallographic studies on the structure of retinal isoforms, computational approaches were taken to model the structure and intermolecular interactions of the mentioned isoforms emphasizing the role of terminal extensions. Using the insights obtained, we aimed to explore suitable sites on the structure of IMPDH for targeting by drugs, to alleviate the role of retinal IMPDH1 in RP by adopting an appropriate pharmacotherapeutics strategy.

## MATERIALS AND METHODS

### *Chemicals and reagents*

Restriction endonucleases, DNA ligase, Pfu polymerase,  $\alpha$ -chymotrypsin, DNA ladder and protein size marker were purchased from Thermo Scientific (USA). All other chemicals used were obtained from Merck (Germany) or Sigma (USA).

### *Cloning and expression of 604-aa isoform lacking C-terminal peptide*

Using the previously cloned sequence of the 604-aa isoform, the desired nucleotide sequence of the 604-aa isoform lacking the C-terminal peptide (the  $\Delta C$  isoform) was amplified with Pfu polymerase, using the forward primer including NdeI restriction site: 5'-GGAATTCATATGGAGGAACCGCTCTCACC-3', and the reverse primer including XhoI restriction site: 5'-CCGCTCGAGAAACGGCAGAAAGGTATAGG-3'. The amplified polymerase chain reaction (PCR) products were cloned into a pET26b+ vector. The accuracy of the sequence was assessed and confirmed by DNA sequencing using T7 promoter and T7 terminator primers. The cloned constructs were transformed

into *E. coli* strain BL21 (DE3) and inoculated into 100 mL of Luria Bertani (LB) medium containing 30 µg/mL kanamycin. Induction was initiated by the addition of 1 mM isopropyl-β-D-thiogalactopyranoside (IPTG). The mixture was kept at 20 °C for 5 h while shaking at 200 rpm. Harvested cells were stored at -70 °C.

#### **Purification of recombinant proteins**

Frozen cell pellets were thawed and resuspended in 3-4 mL of lysis buffer (50 mM NaH<sub>2</sub>PO<sub>4</sub>, 300 mM NaCl, 10 mM imidazole). Lysozyme with the final concentration of 30 mg/mL was added to the bacterial suspension, and incubated on ice for 30 min. The suspension was sonicated and centrifuged for 30 min at 17000 g and 4 °C. The resultant supernatant was applied to the Ni-NTA column, and the recombinant protein was purified following the manufacturer's protocol. The protein quantity was analyzed using Lowry's method (17) with bovine serum albumin as the standard.

#### **Proteolytic digestion**

Proteolysis of the protein samples was performed using a 1:100 molecular weight ratio of α-chymotrypsin (0.5 µg) and the protein (50 µg), in the elution buffer (500 mM imidazole, 300 mM NaCl, and 50 mM Na<sub>2</sub>HPO<sub>4</sub>). To each reaction (total volume of 200 µL), 2 µL of 10% sodium dodecyl sulphate (SDS) was added to stop the proteolysis in 0, 2, 4, 6, 8, 10, and 15 min time points. Then, the protein content of each reaction was precipitated by adding 10 µL of 3 M KCl followed by centrifugation for 5 min at 15000 g. The resulting precipitate was dissolved in 1× SAS polyacrylamide gel electrophoresis (SDS-PAGE) loading buffer and subsequently analyzed by a 10% SDS-PAGE. Band analysis and estimation of protein amounts in the SDS-PAGE gels were performed by the software ImageJ.

#### **Molecular dynamic simulations**

Models of the engineered protein were built by eliminating the 32-aa C-terminal extension peptide of the 604-aa isoform structure obtained from a previous study modelling monomer and

octamers of the retinal isoforms (14). A dimer structure composed of upper and lower monomers of the convex octamer of IMPDH1 was utilized to discover the interactions between the core protein and the peptide extensions both intra-molecular and inter-molecular. Using Gromacs 2019.1 simulation package (18) and CHARMM36 force field (19), these models were subjected to molecular dynamics (MD) simulation. First, the structures were solvated with the TIP3P water model (20) in a cubic box, with a 1 nm distance between the protein and the box edges.

The system was neutralized by adding sufficient counter-charge ions. Energy minimization of the system was performed by the steepest descent method (21). This was followed by 200 ps of MD simulation in the canonical ensemble using the Berendsen thermostat algorithm (22) to increase the temperature of the system to 300 K, and an additional 200 ps of equilibration under isothermal-isobaric conditions with the Parrinello-Rahman algorithm (23). The production run was implemented for 20 ns, which is sufficient to relax the residue positions. Root mean squared deviation (RMSD) and root mean squared fluctuation (RMSF) analyses were performed using Gromacs tools. The interactions of N- and C-terminal peptides were explored visually by UCSF Chimera (24). Secondary structures were calculated using the PolyView-2D web tool.

## **RESULTS**

#### **Recombinant production of ΔC 604-aa isoform**

The IMPDH1 recombinant 604-aa isoform lacking the C-terminal 32-aa peptide was overexpressed in *E. coli* strain BL21 (DE3) in a pET26b+ vector. A poly-histidine tag was located at the C-terminal of the desired protein. PCR sequencing of the recombinant vector with T7 promoter and T7 terminator primers confirmed the accuracy of the target gene. The optimum expression of both the wild type and the modified recombinant proteins were reached at 1 mM IPTG, and shaking for 5 h at 20 °C.

### Proteolytic digestion

To study the fluctuations in the structure of wild type and recombinant  $\Delta C$  604-aa isoforms, protease digestion was carried out. The results have been shown in Fig. 1, where the molecular weight of wild-type IMPDH1 is 64 kDa. Protein bands with molecular weight lower than 35 kDa are the products of digestion. Smaller peptides in the range of 25 kDa did not appear due to limited concentration, further proteolysis, or the applied precipitation protocol. The figure indicates different mobility patterns for the two digested samples. For the engineered protein, the bands occurred faster and about 16% of the protein was digested within the first 2 m, thus much more digested fragments (molecular weight < 35 kDa) were formed relative to the wild type. This could be interpreted as increased flexibility and looseness of the structure due to the elimination of the C-terminal fragment which leads to more accessibility to  $\alpha$ -chymotrypsin.

### MD simulations

MD simulation was utilized in order to obtain a mere understanding of the internal interactions of the C- and N-terminal peptides with the core domains, and the interactions of the C- and N-terminal peptides with the neighbouring protomer in the convex octamer of IMPDH1. The analysis was performed and compared between the engineered  $\Delta C$  and the wild type 604-aa isoform. To evaluate the stability and flexibility, RMSD and RMSF were calculated. The RMSD of all structures converged after 10 ns and stayed stable for the remaining time of the MD simulation.

The average and standard deviations of RMSD in the second half of the MD simulation were  $0.7 \pm 0.05$  and  $0.9 \pm 0.03$  nm, respectively for the wild type and the recombinant IMPDH1. This suggests that the systems, i.e. dimers of both the wild type and the engineered protein, reached an equilibrium state after 10 ns (Fig. 2A). Structural inspection of the MD trajectories showed that the C-ter peptide in the wild type extended the C-terminus of the enzyme toward the C-terminal face of the catalytic barrel, while the N-terminal segment oriented toward the N-terminal face. To investigate the mean residual movement with time, the RMSF was calculated for each residue (Fig. 2B). As expected, the amino and carboxyl-terminal residues of both protein dimers showed higher values than other protein regions. Although lacking the extended C-terminal peptide, the carboxyl-terminal region of  $\Delta C$  IMPDH1 showed a similar degree of mobility compared to that of the wild-type protein (mean RMSF of 0.55 vs 0.38 nm, respectively; Fig. 2B). The RMSF of the N-terminal of the engineered protein was higher in comparison with the wild type (mean RMSF of 0.85 vs 0.36 nm, respectively), suggesting that in the absence of the C-terminal peptide, the restriction of movement on the N-terminal is eliminated. Despite the more fluctuations observed in the N-terminal of the engineered protein, the average mobility of its finger domain region (residues 450-500), including in its catalytic flap, declined (Fig. 2B). This observation might point to a possible internal interaction between the catalytic flaps in the absence of the C-terminal peptides.

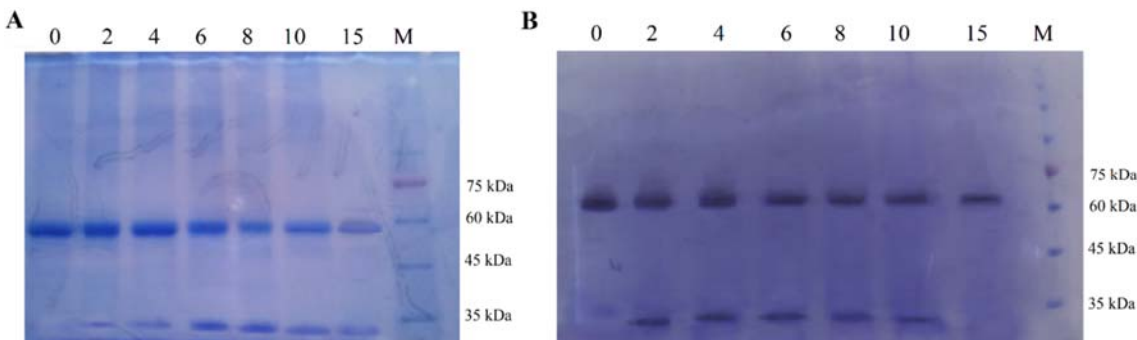


**Fig. 1.** Proteolysis of (A) wild type and (B)  $\Delta C$  engineered 604-aa IMPDH1 isoforms. The proteolytic digestion was followed for 0, 2, 4, 6, 8, 10 and 15 min. IMPDH1; Inosine 5'-monophosphate dehydrogenase isoform 1;  $\Delta C$ , the 604-aa isoform lacking the C-terminal peptide.

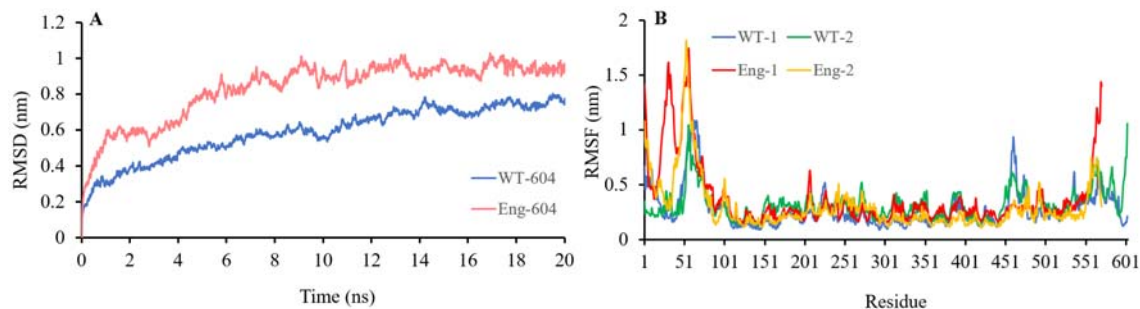


**Fig. 2.** RMSD and RMSF plots for wild type and engineered retinal IMPDH1 modelled as dimers. (A) RMSD plot of the wild type (WT-604) and engineered protein (Eng-604); (B) RMSF plot for individual protomers of wild type (WT-1 and WT-2) and engineered (Eng-1 and Eng-2) dimers. RMSD, Root mean squared deviation; RMSF, root mean squared fluctuation; IMPDH1, inosine 5'-monophosphate dehydrogenase isoform 1.

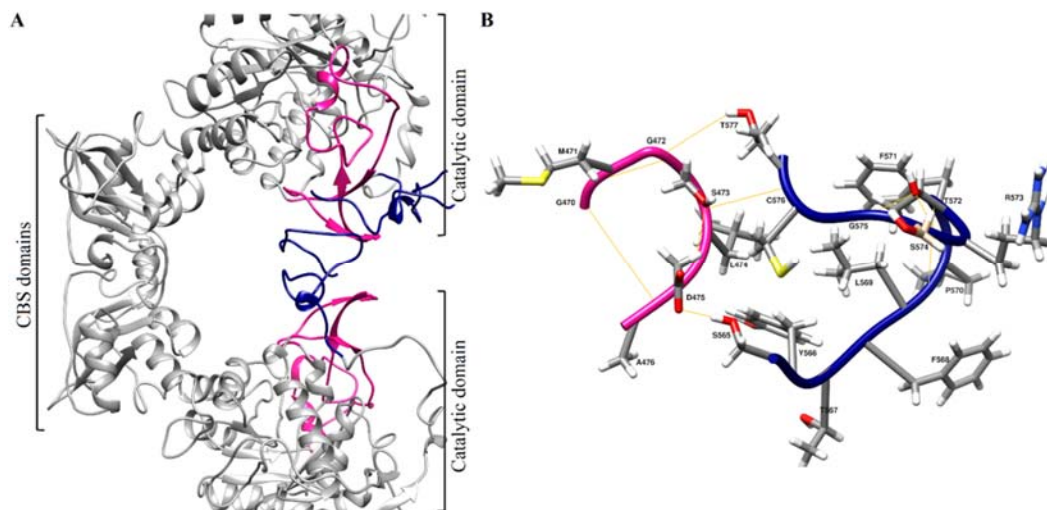


**Fig. 3.** Interactions between catalytic flap (magenta) and C-terminal peptides (blue) of distinct wild type 604-aa isoforms. (A) Overall view of interactions between dimers; (B) detailed view of hydrogen bonds between C-terminal peptide and catalytic flap of distinct monomers. Hydrogen bonds formed between T577, C576, and S565 of the C-terminal peptide and G472, S473, and D475 of the catalytic flap, respectively. To simplify the visualization of interactions, the N-terminal peptide was omitted.

**C-terminal peptide interactions**

During the MD simulation, various interactions between terminal peptides and catalytic flaps of both 604-aa isoform monomers were observed. Because of the disordered nature of these terminal extensions, the interaction of the carboxyl-terminal of one monomer with the N-terminal, catalytic flap, and C-terminal peptide of the opposite monomer was not unexpected. As shown in Fig. 3A, the C-terminal of one monomer, throughout MD simulation, was extended and reached the catalytic flap of the opposing monomer, while still partly covering the catalytic flap of the same monomer. This interaction only occurred in the lower monomer, and the carboxyl-terminal segment of the upper monomer did not

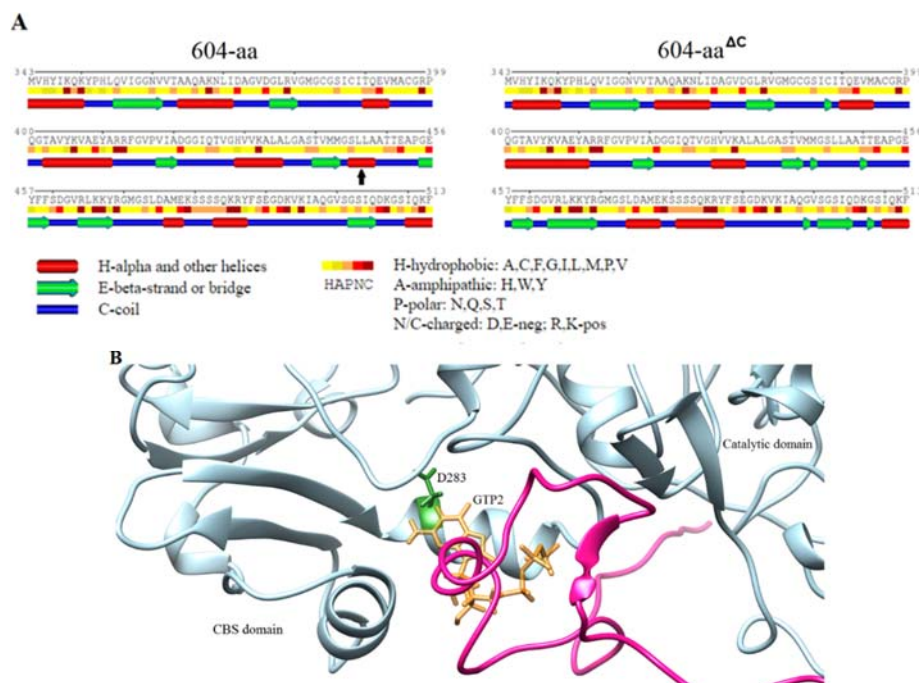
extend to contact the catalytic flap of the adjacent monomer. Instead, consistent with the low RMSF of the catalytic flaps, the C-terminal of the upper monomer masked the catalytic flap of the same monomer, which may restrain its mobility.

Figure 3B illustrates the detailed interactions between the C-terminal and catalytic flap of distinct 604-aa isoform monomers. Hydrogen bonds (H-bonds) formed between Gly472, Ser473, and Asp475 of the catalytic flap and Thr577, Cys576, and Ser565 of the C-terminal peptide of the opposite monomer, respectively. These interactions might highlight the possible role of the C-terminal peptide in the attenuation of the catalytic activity among retinal isoforms.

The communication of the finger domain with the C-terminal could affect enzyme regulation. The interacting residues are neighbours to the IMP binding site and located in the long loop connecting the twisted  $\beta$ -sheet to the catalytic flap. Thus, the C-terminal peptide can extensively affect the whole finger domain because of its flexible nature. This could lead to an altered and unstable position of the finger domain in comparison with that in the canonical variant, probably accounting for the increased rigidity and the diminished inhibitory effect of GDP/GTP in C-terminal-bearing variants, as reported before. We also observed that a small helix formed upstream of the finger domain (residues 446-449). As shown in Fig. 4A, the new secondary structure was not induced in the absence of the C-terminal extension; thus, it can be attributed to the C-terminal peptide and may impose effects on the function of the finger domain. Secondary structural alterations induced by the C-terminal segment were also observed in the N-terminal peptide of the enzyme, where the lack of a carboxyl-terminal extension led to the formation of a new helix with possible effects on the GTP2 binding site (Fig. 4B).

Our analysis of contact counts showed an average of 43 H-bonds and 6 salt bridges for the C-terminal with the protein core, while the N-terminal peptide formed a mean of 46 H-bonds and 12 ionic interactions with the IMPDH1 core protein. Thus, the isoform bearing the N-terminal peptide is expected to be more stable than the 546-aa retinal isoform, indicating that the N-terminal extension of the 604-aa isoform may represent a higher structural impact than the C-terminal one.

As mentioned in the previous sections, interactions between the C- and N-terminal peptides of the 604-aa isoform within the same monomer were observed. These included a hydrogen bond between Glu2 of the N-terminal peptide and Arg592 of the C-terminal peptide and another between Glu2 and Gly593 (Fig. 5A). This explains the lower values of RMSF in the N-terminal of the wild type 604-aa isoform compared to those lacking the C-terminal extension. We have already reported the contact between Glu10 and Arg398 (14). Along with this finding, interactions between the amino-terminal peptide and the rest of the protein were not observed.



**Fig. 4.** (A) Secondary structural illustration for IMPDH1 604-aa isoform in its wild type (left) and  $\Delta C$  engineered (right) forms. A new helix (marked with an arrow) was formed in the wild type, but not in the absence of a C-terminal peptide in the  $\Delta C$  recombinant; (B) formation of a short helix in the GTP2 binding site. Magenta: N-terminal peptide; green: Asp283; orange: GTP. IMPDH1; Inosine 5'-monophosphate dehydrogenase isoform 1;  $\Delta C$ , the 604-aa isoform lacking the C-terminal peptide; GTP, guanosine triphosphate; CBS, cystathione  $\beta$ -synthase.

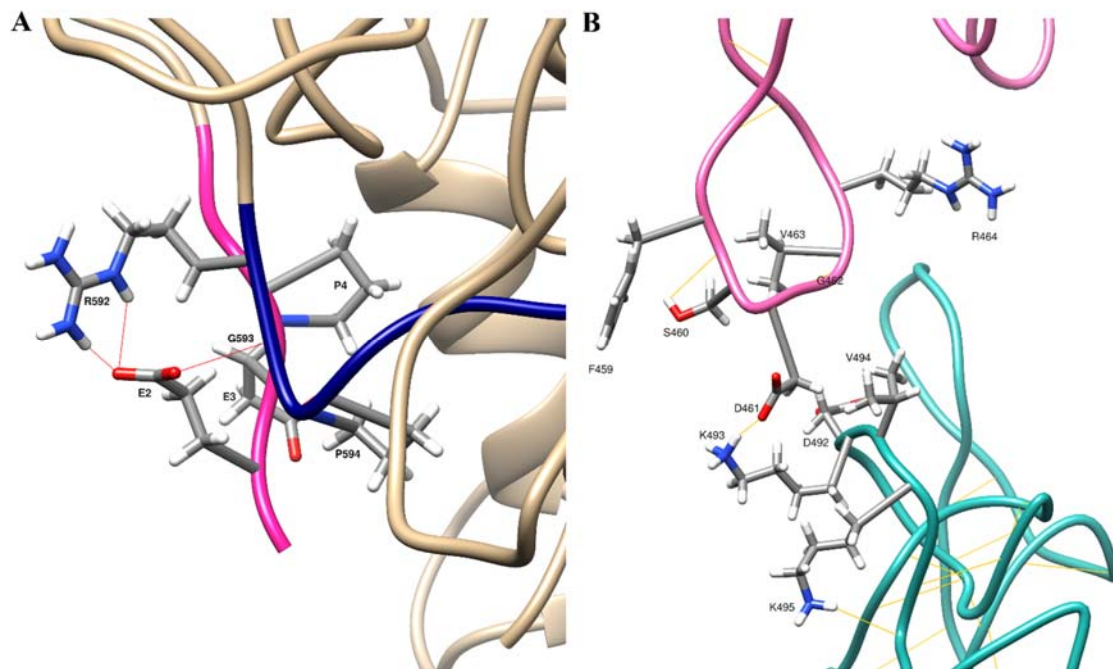


**Fig. 5.** (A) Interactions of N- and C-terminal peptides within the same monomer of wild type 604-aa isoform (magenta: N-terminal peptide and blue: C-terminal peptide); (B) catalytic flaps (magenta and cyan) of distinct monomers of the engineered protein interact in the absence of the C-terminal peptide.

### ***Interactions in the absence of the C-terminal peptide***

Catalytic flaps demonstrated higher flexibility when not restricted by the presence of the C-terminal. For short periods of time along the simulation, catalytic flaps of the engineered monomers were observed to interact. These interactions resulted in the formation of an H-bond between Lys493 and Asp461 of the catalytic flaps of the upper and lower monomers (Fig. 5B). This interaction lasted for the majority of the simulation time, leading to a lower RMSF value of the catalytic flap in comparison with the wild-type isoform, in which the corresponding domains were involved in flexible contacts with the C-terminal peptides.

By eliminating the C-terminal-induced restraint in N-terminal peptide mobility in the  $\Delta C$  604-aa isoform, the N-terminal peptide extended and formed a short helix in the hinge connecting the CBS and the catalytic domains, with this occurring in both monomers. Even though no hydrogen bond formed between the newly formed helix of the N-terminal and other parts of the protein, the N-terminal peptide tended to occupy the binding site of GTP2 (Fig. 4B). The D283N mutation (equivalent to

D226N in human canonical numbering), which is located in this binding site, has been identified to contribute to the occurrence of RP symptoms. Given the importance of this binding site, it might be suggested that in the absence of a C-terminal peptide, the N-terminal extension could play a regulatory role in the catalytic activity of the 604-aa isoform of IMPDH1.

## **DISCUSSION**

IMPDH1, which balances the adenine and guanine nucleotide pool sizes, is a housekeeping enzyme, however, the expression of its canonical isoform in photoreceptors is undetectable (2,3,25). IMPDH1 mutational phenotypes in RP are specific to the retinal tissue, which is primarily attributed to alternative splicing of the gene *RP10* producing two retinal isoforms of the enzyme (1,4,5). Though some research works report the catalytic activity to be indistinguishable among canonical and retinal isoforms (26), other studies have shown their varied catalytic activity and mode of inhibition and have suggested a possible role of terminal extensions (14,27-30). While there is growing research on

this undiscovered role and its connection with RP, the current knowledge about the significance of each domain in the enzyme's overall activity is still limited.

The present study adopted a combination of computational biochemistry and experimental engineering (31-33) to investigate the potential interactions of the N-terminal peptide and the resultant conformational changes. We performed proteolysis on a recombinant 604-aa isoform lacking a C-terminal peptide and simulated the molecular dynamics of its modelled dimer. Our results confirmed previous computational and structural studies (14). Moreover, the formation of a novel short helix in the N-terminal of the engineered protein has been suggested.

Proteolytic digestion of the investigated proteins with  $\alpha$ -chymotrypsin resulted in a time-dependent intensification of SDS-PAGE bands in which the engineered protein digested bands appeared faster than the wild-type isoform. This observation indicates that the 3D conformation of the engineered protein leads to higher accessibility of the protease to digestion sites. Since both experiments produced peptides with similar molecular weights, it can be concluded that the C-terminal peptide covers the digestion site.

Consistent with previous studies (11,12,14), the present research revealed an interaction between catalytic flaps in the  $\Delta$ C recombinant IMPDH1. This interaction could be taken as the cause of the lower RMSF value and hence higher rigidity of the catalytic flap regions in comparison with those in the wild-type dimer. Although the C-terminal peptide restricted the mobility of catalytic flaps, still, higher freedom in movement is observed than the corresponding residues in the engineered protein. It can be concluded that this interaction is favorable and a potent cause of the lower rate of catalytic activity in the naturally existing 604-aa isoform of the enzyme.

Mutations identified in nucleotide binding sites cause RP symptoms. Previous studies have identified three nucleotide binding sites in the regulatory CBS domain of IMPDH (12). In a recent study, an anti-inhibitory role was proposed for the N-terminal peptide of *Homo sapiens* 595-aa isoform. The N-terminal

peptide was suggested to prevent the full inhibition of the enzymatic activity even in the presence of GTP molecules (15). This behavior has been interpreted to be relevant to the IMPDH filament assembly (15). Our computational results suggest that in the absence of a C-terminal peptide, Ala23-Glu28 (604-aa isoform numbering) forms a helix in the second nucleotide binding site. Since we found no direct interactions between the CBS subdomain and the N-terminal peptide, this observation might suggest (a) the masking of the inhibition site which results in higher activity due to the GTP binding prohibition, or (b) a GTP-independent inhibition of the enzyme such as attenuating the filamentation events by covering the outer surface of octamers, as we have suggested earlier (34). These hypotheses remain to be studied further.

Previous studies have shown that the C-terminal peptide is crucial for the function of retinal IMPDH1 (25,35). Our study confirmed that this segment is important, at least because of its digestion-protective role. In addition, the N-terminal peptide contributes to an important anti-inhibitory role. Due to the close proximity of this peptide to the CBS domain, this role may be disrupted with RP-associated mutations. Therefore, to alleviate the detrimental effects of the mutations, augmenting the anti-filamentation role of the N-terminal peptide seems to be an appropriate strategy for treating RP. This can be achieved by designing small-molecule inhibitors binding to the filament assembly surface of IMPDH1 octamers.

## CONCLUSION

The proteolytic digestion of both native 604-aa and the engineered  $\Delta$ C isoforms indicated the protective role of the C-terminal peptide against the proteolysis of the enzyme. Moreover, our computational results revealed the formation of a unique helix in the N-terminal extension. Even though a 604-aa isoform lacking C-terminal is not naturally expressed in photoreceptor cells, in case of elimination of the restricting effect of this terminal peptide on N-terminal extension, an internal inhibition of activity is assumed. The accuracy of this hypothesis remains to be tested.

Putting our findings and previous studies together, targeting the filament assembly interface of IMPDH1 octamers by small-molecule inhibitors seems to be a suitable pharmacotherapeutic approach to treat RP.

### Acknowledgments

This research was financially supported by the Research Council of the University of Tehran; Iranian National Science Foundation (INSF) through Grant No. 94020269 and Deputy of Research and Tech. of Kermanshah University of Medical Sciences through Grant No. 980395.

### Conflict of interest statement

The authors declared no conflict of interest in this study.

### Authors' contributions

All authors contributed to the study conception and design, material preparation, data collection, and analysis. P. Elyasi-Ebli wrote the first draft of the manuscript revised by S. Gharaghani, R. Yazdanparast, and E. Barzegari. All authors read and approved the finalized article.

## REFERENCES

- Bowne SJ, Sullivan LS, Mortimer SE, Hedstrom L, Zhu J, Spellacy CJ, *et al.* Spectrum and frequency of mutations in IMPDH1 associated with autosomal dominant retinitis pigmentosa and leber congenital amaurosis. *Invest Ophthalmol Vis Sci.* 2006;47(1):34-42. DOI: 10.1167/iovs.05-0868.
- Majd N, Sumita K, Yoshino H, Chen D, Terakawa J, Daikoku T, *et al.* A review of the potential utility of mycophenolate mofetil as a cancer therapeutic. *J Cancer Res.* 2014;2014(6):1-12. DOI: 10.1155/2014/423401.
- Hedstrom L. IMP dehydrogenase: structure, mechanism, and inhibition. *Chem Rev.* 2009;109(7):2903-2928. DOI: 10.1021/cr900021w.
- Spellacy CJ, Xu D, Cobb G, Hedstrom L, Bowne SJ, Sullivan LS, *et al.* Investigating the mechanism of disease in the RP10 form of retinitis pigmentosa. *Adv Exp Med Biol.* 2010;664:541-548. DOI: 10.1007/978-1-4419-1399-9\_62.
- Baykov AA, Tuominen HK, Lahti R. The CBS domain: a protein module with an emerging prominent role in regulation. *ACS Chem Biol.* 2011;6(11):1156-1163. DOI: 10.1021/cb200231c.
- Hedstrom L. The dynamic determinants of reaction specificity in the IMPDH/GMPR family of ( $\beta/\alpha$ ) (8) barrel enzymes. *Crit Rev Biochem Mol Biol.* 2012;47(3):250-263. DOI: 10.3109/10409238.2012.656843.
- Glanser ME, Gerlt JA, Babbitt PC. Evolution of enzyme superfamilies. *Curr Opin Chem Biol.* 2006;10(5):492-497. DOI: 10.1016/j.cbpa.2006.08.012.
- Soskine M, Tawfik DS. Mutational effects and the evolution of new protein functions. *Nat Rev Genet.* 2010;11(8):572-582. DOI: 10.1038/nrg2808.
- Labesse G, Alexandre T, Vaupr e L, Salard-Arnaud I, Him JL, Raynal B, *et al.* MgATP regulates allostery and fiber formation in IMPDHs. *Structure.* 2013;21(6):975-985. DOI: 10.1016/j.str.2013.03.011.
- Min D, Josephine HR, Li H, Lakner C, MacPherson IS, Naylor GJ, *et al.* An enzymatic atavist revealed in dual pathways for water activation. *PLoS Biol.* 2008;6(8):e206,1-9. DOI: 10.1371/journal.pbio.0060206.
- Buey RM, Ledesma-Amaro R, Vel azquez-Campoy A, Balsera M, Chagoyen M, de Pereda JM, *et al.* Guanine nucleotide binding to the Bateman domain mediates the allosteric inhibition of eukaryotic IMP dehydrogenases. *Nat Commun.* 2015;6:8923,1-11. DOI: 10.1038/ncomms9923.
- Buey RM, Fern andez-Justel D, Marcos-Alcalde  , Winter G, G omez-Puertas P, de Pereda JM, *et al.* A nucleotide-controlled conformational switch modulates the activity of eukaryotic IMP dehydrogenases. *Sci Rep.* 2017;7(1):2648,1-12. DOI: 10.1038/s41598-017-02805-x.
- Johnson MC, Kollman JM. Cryo-EM structures demonstrate human IMPDH2 filament assembly tunes allosteric regulation. *Elife.* 2020;9:e53243,1-27. DOI: 10.7554/eLife.53243.
- Andashti B, Yazdanparast R, Barzegari E, Galehdari H. The functional impact of the C/N-terminal extensions of the mouse retinal IMPDH1 isoforms: a kinetic evaluation. *Mol Cell Biochem.* 2020;465(1-2):155-164. DOI: 10.1007/s11010-019-03675-9.
- Burrell AL, Nie C, Said M, Simonet JC, Fern andez-Justel D, Johnson MC, *et al.* IMPDH1 retinal variants control filament architecture to tune allosteric regulation. *Nat Struct Mol Biol.* 2022;29(1):47-58. DOI: 10.1038/s41594-021-00706-2.
- Nimmessgern E, Fox T, Fleming MA, Thomson JA. Conformational changes and stabilization of inosine 5'-monophosphate dehydrogenase associated with ligand binding and inhibition by mycophenolic acid. *J Biol Chem.* 1996;271(32):19421-19427. DOI: 10.1074/jbc.271.32.19421.
- Waterborg JH, Matthews HR. The Lowry method for protein quantitation. *Methods Mol Biol.* 1994;32:1-4. DOI: 10.1385/0-89603-268-X:1.
- Van der Spoel D, Lindahl E, Hess B, Groenhof G, Mark AE, Berendsen HJC. GROMACS: fast,

- flexible, and free. *J Comput Chem.* 2005;26(16):1701-1718.  
DOI: 10.1002/jcc.20291.
19. Huang J, MacKerell Jr AD. CHARMM36 all-atom additive protein force field: validation based on comparison to NMR data. *J Comput Chem.* 2013;34(25):2135-2145.  
DOI: 10.1002/jcc.23354.
  20. Koder Hamid M, Månsson LK, Meklesh V, Persson P, Skepö M. Molecular dynamics simulations of the adsorption of an intrinsically disordered protein: force field and water model evaluation in comparison with experiments. *Front Mol Biosci.* 2022;9:958175,1-14.  
DOI: 10.3389/fmolb.2022.958175.
  21. Haug EJ, Arora JS, Matsui K. A steepest-descent method for optimization of mechanical systems. *J Optim Theory Appl.* 1976;19(3):401-424.  
DOI: 10.1007/bf00941484.
  22. Berendsen H, Postma J, van Gunsteren W, DiNola A, Haak J. Molecular dynamics with coupling to an external bath. *J Chem Phys.* 1984;81(8):3684-3690.  
DOI: 10.1063/1.448118.
  23. Parrinello M, Rahman A. Polymorphic transitions in single crystals: a new molecular dynamics method. *J Appl Phys.* 1981;52(12):7182-7190.  
DOI: 10.1063/1.328693.
  24. Yang Z, Lasker K, Schneidman-Duhovny D, Webb B, Huang CC, Pettersen EF, *et al.* UCSF Chimera, MODELLER, and IMP: an integrated modeling system. *J Struct Biol.* 2012;179(3):269-278.  
DOI: 10.1016/j.jsb.2011.09.006.
  25. Gunter JH, Thomas EC, Lengefeld N, Kruger SJ, Worton L, Gardiner EM, *et al.* Characterization of inosine monophosphate dehydrogenase expression during retinal development: differences between variants and isoforms. *Int J Biochem Cell Biol.* 2008;40(9):1716-1728.  
DOI: 10.1016/j.bioce.2007.12.018
  26. Xu D, Cobb G, Spellicy C, Bowne SJ, Daiger SP, Hedstrom L. Retinal isoforms of inosine 5-monophosphate dehydrogenase type 1 are poor nucleic acid binding proteins. *Arch Biochem Biophys.* 2008;472(2):100-104.  
DOI: 10.1016/j.abb.2008.02.012.
  27. Plana-Bonamaisó A, López-Begines S, Fernández-Justel D, Junza A, Soler-Tapia A, Andilla J, *et al.* Post-translational regulation of retinal IMPDH1 *in vivo* to adjust GTP synthesis to illumination conditions. *Elife.* 2020;9:e56418,1-31.  
DOI: 10.7554/eLife.56418
  28. Thomas EC, Gunter JH, Webster JA, Schieber NL, Oorschot V, Parton RG, *et al.* Different characteristics and nucleotide binding properties of inosine monophosphate dehydrogenase (IMPDH) isoforms. *PLoS One.* 2012;7(12):e51096,1-14.  
DOI: 10.1371/journal.pone.0051096
  29. Mortimer SE, Hedstrom L. Autosomal dominant retinitis pigmentosa mutations in inosine 5'-monophosphate dehydrogenase type I disrupt nucleic acid binding. *Biochem J.* 2005;390(Pt 1):41-47.  
DOI: 10.1042/BJ20042051.
  30. Wang XT, Mion B, Aherne A, Engel PC. Molecular recruitment as a basis for negative dominant inheritance? Propagation of misfolding in oligomers of IMPDH<sub>1</sub>, the mutated enzyme in the RP10 form of retinitis pigmentosa. *Biochim Biophys Acta.* 2011;1812(11):1472-1476.  
DOI: 10.1016/j.bbadi.s.2011.07.006.
  31. Seyedhosseini Ghaheh H, Ganjalikhany M, Yaghmaei P, Pourfarzam M, Mir Mohammad Sadeghi H. Improving the solubility, activity, and stability of reteplase using *in silico* design of new variants. *Res Pharm Sci.* 2019;14(4): 359-368.  
DOI: 10.4103/1735-5362.263560.
  32. Fassihi A, Hasanzadeh F, Movahedian Attar A, Saghale L, Mohammadpour M, Mir Mohammad Sadeghi H. Improving the solubility, activity, and stability of reteplase using *in silico* design of new variants. *Res Pharm Sci.* 2020;15(6):515-528.  
DOI: 10.4103/1735-5362.301336.
  33. Balaei F, Ansari M, Farhadian N, Moradi S, Shahlaei M. Interactions and effects of food additive dye Allura red on pepsin structure and protease activity; experimental and computational supports. *Res Pharm Sci.* 2021;16(1):58-70.  
DOI: 10.4103/1735-5362.305189.
  34. Andashti B, Yazdanparast R, Motahar M, Barzegari E, Galehdari H. Terminal peptide extensions augment the retinal IMPDH<sub>1</sub> catalytic activity and attenuate the ATP-induced fibrillation events. *Cell Biochem Biophys.* 2021;79(2):221-229.  
DOI: 10.1007/s12013-021-00973-2.
  35. Spellicy CJ, Daiger SP, Sullivan LS, Zhu J, Liu Q, Pierce EA, *et al.* Characterization of retinal inosine monophosphate dehydrogenase 1 in several mammalian species. *Mol Vis.* 2007;13:1866-1872.  
PMID: 17960124.